Interaction between Solid Surfaces in a Melt of End-Functionalized Polymers

Jijun Wang, Rüdiger Stark, Michael Kappl, and Hans-Jürgen Butt*

Max-Planck-Institute for Polymer Research, Ackermannweg 10, 55128 Mainz, Germany

Received October 27, 2006; Revised Manuscript Received February 1, 2007

ABSTRACT: Using atomic force microscopy, the force between solid surfaces (oxidized silicon) was studied in a melt of end-functionalized polymers (hydroxyl-terminated polyisoprene). The surfaces repelled each other in both approach and retraction. Comparison to results obtained with methyl-terminated polyisoprene shows that the hydroxyl groups bind to the silicon oxide surfaces, and a polymer brush is formed. Thickness and stability of the brush increase with the molecular weight, possibly due to entanglement. With increasing humidity the repulsive force decreases and changes to attraction in the retracting part. This implies that water adsorbs to the interface and destabilizes the bond between the hydroxyl group and the oxidized silicon.

Forces between solid surfaces in polymer melts have been studied theoretically,[1−3] by simulations,[4,5] and experimentally[6−11] because of their fundamental significance for an understanding of confined polymers, of polymers at surfaces, lubrication, and for applications such as making composite materials. Recently, we could confirm one of the theoretical predictions of theory and simulations,[1,2,4] namely, that for a weak polymer−solid surface interaction no long-range force between two solid surfaces should exist. In these experiments the interaction between an atomic force microscope (AFM) tip and a silicon wafer was measured in a melt of polyisoprene (PI).[12] PI interacts weakly with the silicon oxide surface, leading to contact angles around 20°. No significant force was detected at distances larger than 1 nm. Here, we extend these studies by using hydroxyl-terminated PI. To our knowledge, this is the first report on surface forces in melts of end-functionalized polymers.

1,4-Polyisoprene terminated on one end with a hydroxyl group and on the other with a methyl group (PI-OH) and 1,4-polyisoprene terminated on both ends with methyl groups (PI-CH_3) were synthesized by anionic polymerization (cis:trans was 70:30 as determined by NMR). Relative to the critical entanglement molecular weight of PI (M_c = 6.4 kDa),[13] a long- and a short-chain PI were studied (Table 1). To avoid decomposition and water adsorption, the polymers were stored at −7 °C on molecular sieves. As samples, naturally oxidized silicon wafers were used (100, Si-mat Silicon Materials, Landsberg, Germany).

Force−distance curves were measured with an AFM (Multimode, Nanoscope 3, Veeco Instruments, CA) equipped with a PicoForce low-noise head. The polymer was injected between tip and the surface through a liquid cell without O-ring and incubated for 12−15 h either in nitrogen environment or in air with relative humidity of 20−60% at 23 °C. Such a long incubation was chosen because the structure of the polymer at a solid interface can change over several hours.[9,10,14−16] V-shaped silicon nitride cantilevers (length 100 μm, thickness 0.6 μm, Veeco Instruments, Santa Barbara, CA) with integrated tips were used. To determine the tip shape, uncoated, bare tips were imaged with a low-voltage scanning electron microscope (SEM, LEO 1530 Gemini, Oberkochen, Germany). The radii of the tip curvature were in the range of R = 20−60 nm. Cantilever spring constants were 0.2−0.4 N/m as determined by measuring the thermal noise. In a force measurement, the silicon surface was periodically moved up and down at constant velocity while the cantilever deflection was measured. The result is a graph of the cantilever deflection vs the height position of the scanner. From this, force vs distance curves, briefly called "force curves", were calculated by multiplying the cantilever deflection with the spring constant to obtain the force and subtracting the cantilever deflection from the height position to obtain the distance. Zero distance is derived from the linear contact part of force curves, as described in ref 17. This is in fact a critical issue. It is possible and should be kept in mind that actual contact is not established but that a tightly bound polymer layer is still confined between the tip and sample surface. Force curves were taken at a scan size of 200 nm and a frequency of 0.05 Hz either in a nitrogen environment or in air with a humidity of 20−60% at 23 °C. Each force curve contained 512 points on approach and 512 on retraction.

Table 1. Molecular Characteristics of Polyisoprene Terminated with a Hydroxyl or Methyl Group[a]

sample	M_w (kg/mol)	M_w/M_n	N	R_g (nm)	L (nm)
short-chain PI-OH	3.4	1.12	50	1.8	23
long-chain PI-OH	8.7	1.07	128	2.9	58
short-chain PI-CH_3	3.4	1.07	50	1.8	23
long-chain PI-CH_3	8.1	1.09	119	2.8	54

[a] Weight-average molecular weight M_w, polydispersity index M_w/M_n, average number of monomers N, radius of gyration R_g (estimated from R_g^2/M_w = 0.001 nm^2 g^{-1} mol[39,40]), and contour length $L = N\cdot$0.456 nm.

Figure 1A shows a typical force curve of short-chain PI−OH measured in a dry nitrogen environment. For distances below ≈6 nm a repulsive force was observed. In contrast, PI-CH_3 showed no force for distance above 1 nm (Figure 1B). This agrees with earlier experiments.[12] The absence of a force for PI-CH_3 shows that the polymer chain and the methyl end groups only interact weakly with the surfaces of the silicon wafer and the tip; if the polymer binds to the surfaces, repulsive forces are expected.[1,2,4,18] Thus, for PI-OH we can conclude that binding occurs and binding is via the terminal hydroxyl group. The bond is stable on the time scale of one contact (1−5 s).

To analyze the results quantitatively, we applied the model of Doland and Edwards,[19] who calculated the configurational free energy of a random flight polymer chain, which is attached

* Corresponding author: e-mail butt@mpip-mainz.mpg.de, phone 0049-6131-379 111, fax 0049-6131-379 310.

10.1021/ma062484a CCC: $37.00
Published on Web 03/01/2007

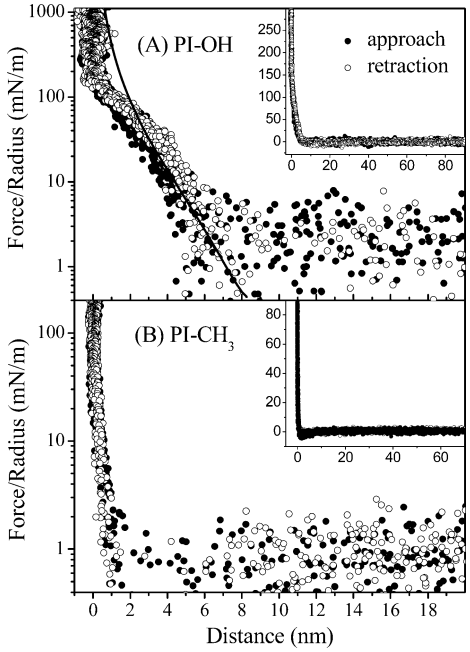

Figure 1. Force curves measured in PI-OH (A: $M_w = 3.4$ kDa) and PI-CH_3 (B: $M_w = 3.4$ kDa) on a silicon wafer with silicon nitride tip in dry nitrogen. Please note the different force scales. Five force curves are superimposed. The inset shows the force curves at a larger scale. Forces were normalized by dividing them by the radius of curvature R of the tips. In this specific example $R = 30$ nm for PI-OH and $R = 44$ nm for PI-CH_3. The continuous line is a fit of the approaching part with eq 1 ($R_g = 1.8$ nm, $\Gamma = 4.4 \times 10^{17}$ m^{-2}).

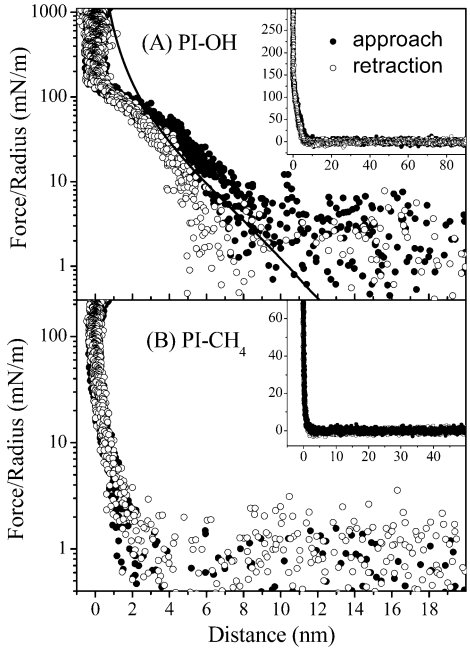

Figure 2. Normalized force curves measured in long-chain PI-OH (A: $M_w = 8.7$ kDa, $R = 28$ nm) and PI-CH_3 (B: $M_w = 8.1$ kDa, $R = 48$ nm) on a silicon wafer with a silicon nitride tip in dry nitrogen. The inset shows a lager scale. The continuous line is a fit with eq 1 ($R_g = 2.9$ nm, $\Gamma = 2.5 \times 10^{17}$ m^{-2}).

at one end to a planar surface, from its number of possible configurations. The free energy per unit area is then derived by multiplication with the number of molecules and division by the area. To convert free energy per unit area w to a force F, we applied Derjaguin's approximation,[20] taking the tip to be spherical at the end with a radius of curvature R: $F = 2\pi Rw$. The validity of this approximation is discussed later. As a normalized force we obtain[19]

$$\frac{F}{R} = 2\pi\Gamma k_B T\left[\ln\left(\frac{D}{4\sqrt{\pi}R_g}\right) + \left(\frac{\pi R_g}{D}\right)^2\right] \quad \text{for } D \le 3\sqrt{2}R_g$$

$$\frac{F}{R} = 4\pi\Gamma k_B T e^{-D^2/4R_g^2} \quad \text{for } D > 3\sqrt{2}R_g \qquad (1)$$

Γ is the number of bound polymer chains per unit area, k_B and T are Boltzmann's constant and temperature, D is the distance, and R_g is the radius of gyration of the polymer. Since the radius of gyration is known, the only fit parameter was the surface density Γ. Alternative expressions for the steric force between polymer brushes in solvents are reported in the literature (e.g. refs 21−23). These, however, take the solvent and the resulting osmotic pressure into account, which should be absent in a melt.

Force curves measured with short-chain PI-OH could be fitted with eq 1 for distances above 2−3 nm using $\Gamma = (1.5\text{ nm})^{-2}$. This is a mean value obtained from fitting approaching force curves. For different experiments and fitting approach and retraction this value ranged from $(1.1\text{ nm})^{-2}$ to $(2.0\text{ nm})^{-2}$. For long-chain PI-OH longer ranged repulsive forces were observed (Figure 2A), which could also be fitted with eq 1 for distances above 3 nm, leading to $\Gamma = (2.0\text{ nm})^{-2}$ (range from $(1.6\text{ nm})^{-2}$ to $(2.7\text{ nm})^{-2}$). With PI-CH_3 only insignificantly low forces were measured (Figure 2B). We interpret the repulsive force as being due to the formation of a brushlike structure of PI-OH at the surface. As predicted for poly(dimethylsiloxane),[24] the terminal

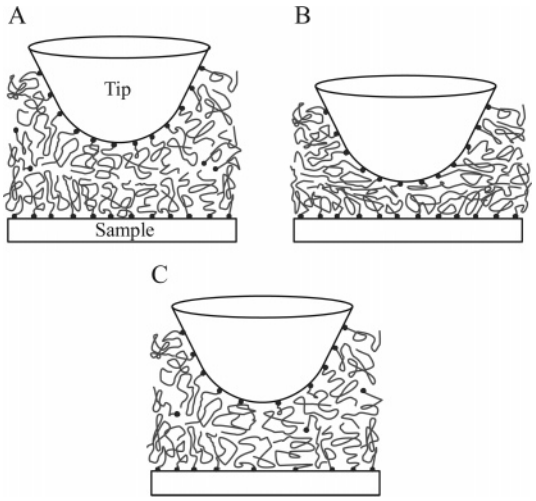

Figure 3. Schematic of the AFM tip and sample in PI-OH at a distance $D \ge 3$ nm where the brushlike layer is compressed (A). For $D < 3$ nm the individual chains escape to the side (B). At high load or induced by adsorbed water part of the brushlike structure is removed (C).

hydroxyl groups strongly bind to the oxidized silicon wafer surface and the oxidized silicon nitride tip surface. A brush formed by polymer chains with an adsorbing end leads to a steric repulsion (Figure 3A).[19,21−23,25−27] To accommodate many hydroxyl groups on the surface, the adsorbed chains will deform from the random coil to a more stretched configuration, which leads to an increased graft density.[28] For PI-CH_3 no brushlike structure was formed, and thus no interaction was observed.

For distances shorter then ≈3 nm the measured force is lower than predicted by eq 1. We attribute this to an "escape transition" of individual chains, which escape the compression of the tip by splaying in radial direction (Figure 3B).[29−31] In this case Derjaguin's approximation and thus eq 1 are not applicable anymore, and the force on a curved tip is qualitatively different from the force between two parallel plates. Please note that such

an escape transition does not imply that the adsorption site of the polymer chain is removed or shifted.

For long-chain PI-OH the shape of force curves did not change significantly when increasing the load (maximal applied force). Maximal normalized loads were 2−4 N/m. Higher loads were not applied to avoid nonlinear effects at high cantilever deflection. Thus, on the time scale of one contact (1−5 s), for the pressures and pressure gradients applied the brushlike structures were stable. We can estimate these pressures using the Hertz model for an elastic sphere interacting with an elastic planar surface.[32] For a Hertz contact the pressure shows a parabolic profile in the circular contact region, $P = P_0(1 - r^2/a^2)$, with a maximal pressure P_0 in the center. The radius of this contact region a is given by $a^3 \approx 3RF/(4E)$. For the Young's modulus E only a lower limit can be given because we cannot be sure whether the silicon wafer and the tip are in direct contact or whether a polymer layer is still confined between the two surfaces. This lower limit is estimated as described previously to be $E \gg 4 \times 10^8$ Pa,[33] which leads to a contact radius of at most 10 nm ($R = 30$ nm, $F = 30$ nN). We get a P_0 of the order of 200 MPa and a maximal pressure gradient of the order of 4×10^{16} Pa/m.

With short-chain PI-OH the repulsive force decreased with increasing load. When extrapolating the repulsive force to zero distance to obtain a "force amplitude", typically 150 mN/m was observed at loads up to 1.2 N/m. When increasing the load to 2 N/m, this force amplitude decreased to typically 110 mN/m. Both approaching and retracting parts of force curves were equally affected by an increase in load, and no hysteresis was observed. The weakening of the repulsive force for short-chain PI-OH with increasing load indicates that structure and density of the brushlike layer are changed by the tip. The decrease in force shows that the density of adsorption sites in the contact region of the tip is reduced (Figure 3C), either by desorption of chains into the bulk or by a lateral shift of binding sites.

This implies that brushes of short-chain PI-OH are less stable than those of long-chain PI-OH despite the fact that they can form a higher density of OH bonds on the surface. An additional stabilization due to entanglement seems to overcompensate this effect and lead to an increased stability. The observation also implies that the formation of the brush in short-chain PI-OH takes longer than 20 s, the interval between two force curves. A decrease of the force was also observed for polymers adsorbed in solution after taking few force curves[34] or after shearing.[35]

All experiments described so far were carried out in a dry environment, and the content of water was reduced as much as possible. Under ambient conditions attractive forces were observed when the load exceeded a certain value. Figure 4 shows typical force curves measured in long-chain PI-OH at different loads in air at a humidity of 60%. Even when applying a low load of only 240 mN/m the repulsion decreased by a factor 2−3 as compared to the dry case (Figure 4A). Approaching and retracting parts of force curves were indistinguishable. However, force curves could not at all be fitted by eq 1. Upon increasing the load to 330 mN/m, an adhesion began to appear in the retraction (Figure 4B). The adhesion further increased with increasing load (Figure 4C). When decreasing the load again, the process was reversible. This behavior was observed for long- and short-chain PI-OH for humidities at or above 40%.

The results demonstrate that water adsorbs to the solid surface−polymer interface. The presence of water decreased the repulsive force and thus the apparent stability of the brush. Two mechanisms are possible. One is a decrease in the thermodynamic adsorption energy of the polymer hydroxyl

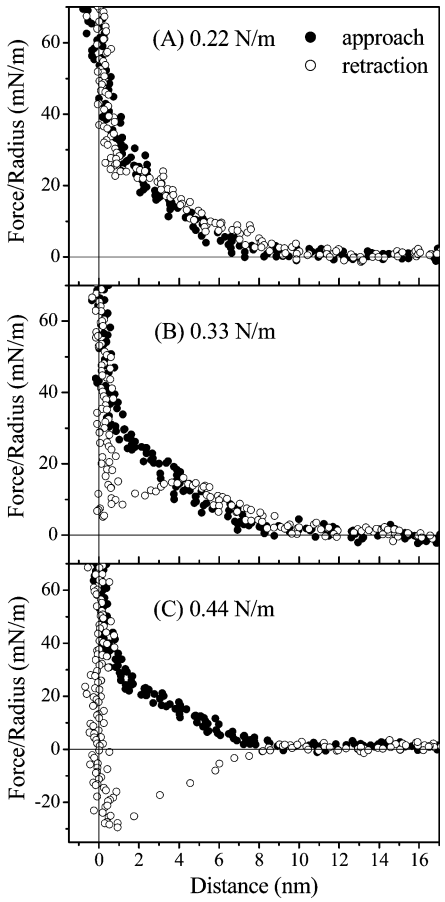

Figure 4. Normalized force curves measured in long-chain PI-OH ($M_w = 8.7$ kDa, $R = 55$ nm) between a silicon wafer and a silicon nitride tip in air at a humidity of 60% at different loads (A, 240 mN/m; B, 330 mN/m; C, 440 mN/m).

groups to the tip and sample surfaces. Water molecules could for example compete for adsorption sites with the polymer hydroxyl groups. Second, adsorbed water can accelerate the kinetics of the binding/desorption of the polymer hydroxyl groups by reducing the activation energy for desorption, for example by changing the effective dielectric constant of the local environment. If the time constant for desorption is reduced below the contact time, polymer chains could laterally move or desorb. An alternative hypothesis to explain the adhesion in retraction is the formation of a water meniscus due to capillary condensation and the resulting capillary force. The reduced Laplace pressure in the meniscus and the surface tension between the polyisoprene and water would cause an attractive capillary force.[20,36−38]

With PI-CH_3 no significant change in the approaching force curves was observed but an adhesion on the retraction. Unfortunately, this observation does not help to discriminate between the two hypothesis. The adhesion could be a capillary force caused by water adsorbed at the interfaces. It could also be the simple fact that an adsorbed layer of water leads to more hydrophilic silicon oxide surfaces, which in the hydrophobic PI have a high tendency to adhere.

Summary and Conclusions

PI-OH binds with its terminal hydroxyl group to the silicon wafer and silicon nitride tip. This results in the formation of brushlike structures and a repulsive force between the two surfaces. The force range and the stability of the brush increased with the molecular weight of the polymer. In the presence of

water vapor, water adsorbs to the silicon oxide−polymer interface, weakens the bond between the hydroxyl group and the solid surface, and reduces the repulsive force.

Acknowledgment. We thank X. Ling, D. Wu, M. Wagner, T. Wagner, and J. Thiel for helpful discussions, synthesis, and characterization and the Alexander von Humboldt Foundation for a research fellowship.

References and Notes

(1) de Gennes, P. G. *C.R. Acad. Sci. Paris* **1987**, *305*, 1181−1184.
(2) Ausserré, D. *J. Phys. (Paris*) **1989**, *50*, 3021−3042.
(3) Subbotin, A.; Semenov, A.; Hadziioannou, G.; ten Brinke, G. *Macromolecules* **1996**, *29*, 1296−1304.
(4) ten Brinke, G.; Ausserre, D.; Hadziioannou, G. *J. Chem. Phys.* **1988**, *89*, 4374−4380.
(5) Müller, M.; Binder, K.; Albano, E. V. *Int. J. Mod. Phys. B* **2001**, *15*, 1867−1903.
(6) Montfort, J. P.; Hadziioannou, G. *J. Chem. Phys.* **1988**, *88*, 7187−7196.
(7) Horn, R. G.; Hirz, S. J.; Hadziioannou, G.; Frank, C. W.; Catala, J. M. *J. Chem. Phys.* **1989**, *90*, 6767−6774.
(8) van Alsten, J.; Granick, S. *Macromolecules* **1990**, *23*, 4856−4862.
(9) Granick, S.; Hu, H. W. *Langmuir* **1994**, *10*, 3857−3866.
(10) Hirz, S.; Subbotin, A.; Frank, C.; Hadziioannou, G. *Macromolecules* **1996**, *29*, 3970−3974.
(11) Luengo, G.; Heuberger, M.; Israelachvili, J. *J. Phys. Chem. B* **2000**, *104*, 7944−7950.
(12) Stark, R.; Bonaccurso, E.; Kappl, M.; Butt, H. J. *Polymer* **2006**, *47*, 7259−7270.
(13) Fetters, L. J.; Lohse, D. J.; Milner, S. T.; Graessley, W. W. *Macromolecules* **1999**, *32*, 6847−6851.
(14) Evmenenko, G.; Mo, H.; Kewalramani, S.; Dutta, P. *Polymer* **2006**, *47*, 878−882.
(15) Arrighi, V.; Higgins, J. S.; Burgess, A. N.; Floudas, G. *Polymer* **1998**, *39*, 6369−6376.
(16) Sun, G.; Kappl, M.; Pakula, T.; Kremer, K.; Butt, H.-J. *Langmuir* **2004**, *20*, 8030−8034.
(17) Butt, H.-J.; Cappella, B.; Kappl, M. *Surf. Sci. Rep.* **2005**, *59*, 1−152.
(18) Leermakers, F. A. M.; Butt, H.-J. *Phys. Rev. E* **2005**, *72*, 021807.
(19) Dolan, A. K.; Edwards, S. F. *Proc. R. Soc. London A* **1974**, *337*, 509−516.
(20) Derjaguin, B. *Kolloid-Z.* **1934**, *69*, 155−164.
(21) de Gennes, P. G. *Adv. Colloid Interface Sci.* **1987**, *27*, 189−209.
(22) Milner, S. T.; Witten, T. A.; Cates, M. E. *Macromolecules* **1988**, *21*, 2610−2619.
(23) Patel, S.; Tirrell, M.; Hadziioannou, G. *Colloids Surf.* **1988**, *31*, 157−179.
(24) Tsige, M.; Soddemann, T.; Rempe, S. B.; Grest, G. S.; Kress, J. D.; Robbins, M. O.; Sides, S. W.; Stevens, M. J.; Webb, E. *J. Chem. Phys.* **2003**, *118*, 5132−5142.
(25) Ash, S. G.; Findenegg, G. H. *Trans. Faraday Soc.* **1971**, *67*, 2122.
(26) Taunton, H. J.; Toprakcioglu, C.; Fetters, L. J.; Klein, J. *Macromolecules* **1990**, *23*, 571−580.
(27) Klein, J.; Perahia, D.; Warburg, S. *Nature (London)* **1991**, *352*, 143−145.
(28) Kumacheva, E.; Klein, J.; Pincus, P.; Fetters, L. J. *Macromolecules* **1993**, *26*, 6477−6482.
(29) Subramanian, G.; Williams, D. R. M.; Pincus, P. A. *Europhys. Lett.* **1995**, *29*, 285.
(30) Murat, M.; Grest, G. S. *Macromolecules* **1996**, *29*, 8282−8284.
(31) Guffond, M. C.; Williams, D. R. M.; Sevick, E. M. *Langmuir* **1997**, *13*, 5691−5696.
(32) Hertz, H. J. *Reine Angew. Math.* **1882**, *92*, 156−171.
(33) Stark, R.; Kappl, M.; Butt, H.-J. *Chin. Polym. J.*, in press.
(34) Courvoisier, A.; Isel, F.; Francois, J.; Maaloum, M. *Langmuir* **1998**, *14*, 3727−3729.
(35) Eiser, E.; Klein, J.; Witten, T. A.; Fetters, L. J. *Phys. Rev. Lett.* **1999**, *82*, 5076−5079.
(36) Fisher, R. A. *J. Agric. Sci.* **1926**, *16*, 492−505.
(37) Princen, H. M. *J. Colloid Interface Sci.* **1968**, *26*, 249−253.
(38) Farshchi, M.; Kappl, M.; Cheng, Y. H.; Gutmann, J. S.; Butt, H.-J. *Langmuir* **2006**, *22*, 2171−2184.
(39) Faller, R.; Reith, D. *Macromolecules* **2003**, *36*, 5406−5414.
(40) Creton, C.; Brown, H. R.; Shull, K. R. *Macromolecules* **1994**, *27*, 3174−3183.

MA062484A